As Plain as the Nose on Your Face?

Peter A. C. Varley[a], Stefania Cristina[b], Alexandra Bonnici[c] and Kenneth P. Camilleri[d]
Department of Systems and Control Engineering, University of Malta, Msida MSD 2080, Malta

Keywords: Gaze Tracking, Head Pose, Noses, Haar Cascades.

Abstract: We present an investigation into locating nose tips in 2D images of human faces. Our objective is conference-room gaze-tracking, in which a presenter can control a presentation or demonstration by gaze from a distance in the range 2m to 10m. In a first step towards this, we here consider faces in the range 150cm to 300cm. Head pose is the major contributing component of gaze direction, and nose tip position within the image of the face is a strong clue to head pose. To facilitate detection of nose tips, we have implemented a combination of two Haar cascades (one for frontal noses and one for profile noses) with a lower failure rate than existing cascades, and we have examined a number of "hand-crafted ferns" for their potential to locate the nose tip within the nose-like regions returned by our Haar cascades

1 INTRODUCTION

Our objective is conference-room gaze-tracking, in which a presenter can control a presentation or demonstration by gaze from a distance in the range 2m to 10m.

Current gaze-tracking systems typically track the gaze of a computer user, usually seated about 70cm from the camera. Some interactive displays such as (Zhang, 2016) assume that the user is 130cm from the camera. In a first step towards extending this, we consider faces in the range 150cm to 300cm. Many images from the Labelled Faces in the Wild dataset (Huang et al., 2007), such as those in Figure 1, are typical of faces in this range.

There are two components which combine to give a gaze estimate: head pose, and eyeball rotation. In this short paper, we deal only with head pose. The geometry of combining head pose and eyeball rotation to obtain a full gaze vector is well-known - see (for example) (Ishikawa et al., 2004). Readers interested in eyeball rotation and in gaze-tracking in general may wish to consult (Cristina and Camilleri, 2018), and those interested in a comparison of different face-finding methods may wish to consult (Rahmad et al., 2020).

Of the two, head pose is the major contributor, as the head has a wider range of movement than the eyeball, and it is also easier to detect as the head is larger and more visible. We may also wish to allow for a failsafe mode in which we use head pose alone when pupil gaze direction is unavailable - users may even prefer this, as they can control the screen with head pose while making eye contact with their audience.

Head pose can be estimated by locating and combining facial features in an image, but which features should be chosen? Some facial features are not even visible in images from 10m away (irises are a few pixels across at most, and pupils could disappear entirely). And people talk in conference rooms, so mutable features such as the mouth are also unreliable.

The nose is part of the rigid structure of the head - it is possible to gesture with the nose, but people do not typically do so when giving presentations - and it is proverbially the most visible feature of the face. In this paper, we only consider methods which use the nose (possibly in combination with other features) to determine head pose.

Weidenbacher (Weidenbacher et al., 2006) uses ten feature points to determine head pose: three from each eye, the two nostrils, and the corners of the mouth.

Fasthpe (Sapienza and Camilleri, 2014) uses the nose tip and a triangle formed by eyes and mouth to predict head pose. The principal advantage of this over previous methods is that the nose tip is the feature furthest from the plane of the eyes and mouth, so it is more informative about 3D than anything else.

[a] https://orcid.org/0000-0003-4181-9234
[b] https://orcid.org/0000-0003-4617-7998
[c] https://orcid.org/0000-0002-6580-3424
[d] https://orcid.org/0000-0003-0436-6408

Varley, P., Cristina, S., Bonnici, A. and Camilleri, K.
As Plain as the Nose on Your Face?.
DOI: 10.5220/0010315404710479
In *Proceedings of the 16th International Joint Conference on Computer Vision, Imaging and Computer Graphics Theory and Applications (VISIGRAPP 2021) - Volume 4: VISAPP*, pages 471-479
ISBN: 978-989-758-488-6

Figure 1: From LFW (a) Frontal Nose, (b) Profile Nose, (c) Ambiguous Nose.

A further advantage is that there is only one calibration parameter needed, distance of nose tip from eye-mouth plane, and it has an obvious geometric meaning and is easily and unobtrusively determined for a new user. On the other hand, although fitting a tetrahedron to four points is straightforward, it is not robust to bad points.

Our planned system will make use of both eye gaze direction and head pose, and we follow Fasthpe in using the nose tip to determine head pose. For this, we need an accurate position of the nose tip in the image. This paper considers various methods of determining the nose tip position, makes recommendations, and presents preliminary results.

This paper does not discuss how to convert nose tip position to a gaze prediction. This is something we shall test in due course. Options range from simply projecting a vector from a reference point to the nose tip, as in Figure 2, to compiling a feature vector (a list of facial landmarks and their locations) and using this as an auxiliary input to a neural network, as in (Lu and Chen, 2016) and (Zhang, 2016), or even to creating a full 2.5D head model (Caunce et al., 2009).

Ergonomically, any strictly monotonic function which converts a nose tip position to a gaze prediction is potentially satisfactory, and indeed it is possible that users may prefer to make exaggerated gestures rather than geometrically-accurate gestures.

On a practical note: we prefer methods which can be retrained quickly on a portable computer. Should it happen that a demonstration fails in the morning (which is always possible with a prototype), we would wish to gather training data from our potential customers during the coffee break, add this to our training dataset, retrain the system over the lunch break, and demonstrate a working system in the afternoon, all without having to return to the laboratory to use computers with more parallel processing capability but no mobility.

We also prefer methods which are easily replicated: other researchers should be able to reproduce (or even improve on!) our results.

Section 2 describes the characteristics of noses in images of human faces. Section 3 lists and discusses previous work. Section 4 describes our own investigations to date and presents preliminary results. Section 5 presents our conclusions and plans for further development of our ideas.

1.1 Terminology

By convention, left and right are from the user's point of view, so the left eye and left nostril are those on the right of the image.

2 NOSES IN IMAGES

The three images in Figure 1 are taken from the LFW Dataset (Huang et al., 2007). This is a reasonable source of training data: images are 250x250, the face of the subject is usually central, and the size of the face is usually between 60x60 and 130x130 pixels, with the median being 110x110. Such images would be typical of a webcam image of a subject at a distance of between 1.5m and 3m.

We maintain two datasets. Our reference dataset. used for testing, comprises 3007 sample images (1474 female, 1533 male) selected from the LFW dataset such that each image portrays a different person; some images contain additional faces in the background, and where these are detected too, they are included in our test results. Our primary dataset is a subset of 100 images (51 female, 49 male) taken from the reference dataset and used during development - the three images in Figure 1 are among those included in our primary dataset. A total of 502 images, including all of those in the primary dataset, have been fully labelled by eye. Both primary and reference datasets include wide varieties of lighting intensities and directions.

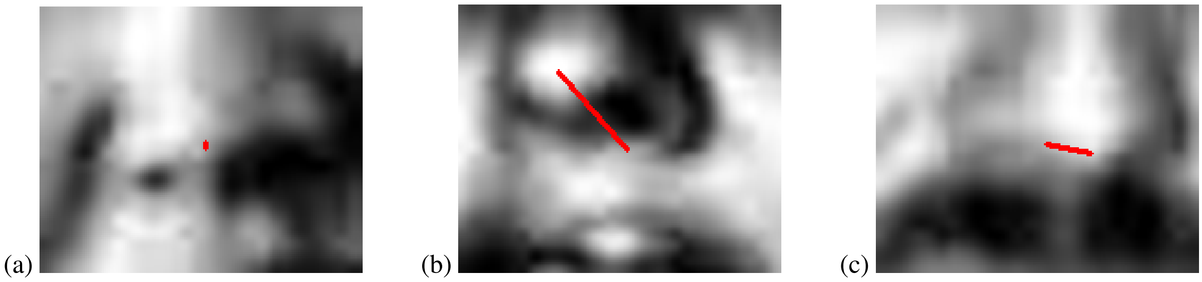

Figure 2: Nose Regions produced by MCS Nose Cascade from images in Figure 1.

It can be seen that in all three the nose gives a good estimation of the head pose, and the head pose gives a good estimation of the gaze. Even in more complex cases where the eye direction and the head pose are not in agreement, the head pose is still the major component of the gaze direction, and we can still obtain a good estimate of it from the nose.

Unlike eyeballs, which are always roughly spherical so present the same appearance from any viewpoint, noses are a peculiar and distinctive shape - frontal noses (e.g. Figure 1a) and profile noses (e.g. Figure 1b) can look very different in 2D images. And what are we to make of Figure 1c, which is mid-way between frontal and profile? Perhaps we can turn this difficulty into an advantage - an accurate assessment of where the nose is pointing will give us a very good estimate of head pose.

3 METHODS

There are several established methods for detecting features in images. Use of *Haar Cascades* is widespread, not least because of their inclusion in OpenCV (OpenCV, 2015). In recent years, *Ferns* (Cao et al., 2012) have become popular.

3.1 Haar Cascades

Haar Cascades were introduced by (Viola and Jones, 2004), who described their innovation as "reminiscent of Haar basis functions", with additions and improvements by (Lienhart and Maydt, 2002), who created one of the most successful cascade classifiers, the "alt2" face detector.

The simplest form of *Cascade Classifier* is a linear sequence of *Stage Classifiers* (Viola and Jones, 2004). The number of Stage Classifiers is specified by the user, and is typically around 20 (OpenCV, 2015), (Castrillón et al., 2007).

Each *Stage Classifier* is a *Haar Feature*, a function which compares the sums of pixel intensities in adjacent rectangles. There are five basic Haar Features (Viola and Jones, 2004): four of these use 2 rectangles; the fifth uses 4. Tilted features at 45° (Lienhart and Maydt, 2002) and symmetrical features can be added if needed. To speed up this process, (Viola and Jones, 2004) introduced "intensity images", two-dimensional arrays in which each element contains the sum of the intensities of pixels above and to the left of that point in the original image; thus, calculating $(TL+BR)-(TR+BL)$ from the four points at the corners of a rectangle in the intensity image gives the sum of all pixels in the the same rectangle in the original image. Haar Features are weighted according to their success at accepting positive samples and rejecting negative samples.

Stages after the first use *Adaptive Boosting* (Viola and Jones, 2004), in which successful Haar Feature/sample results in earlier stages are given a reduced weight when creating later stages, as their job has already been done. Haar Cascades have been used successfully to detect faces in images (OpenCV, 2015) and to detect eyes and mouths in faces (OpenCV, 2015), (Castrillón et al., 2007).

One would think that, as noses are a peculiar and distinctive shape, it should be easy to train Haar cascades to find them, as that is the sort of thing which Haar cascades are good at. It is not so easy in practice. For example, Castrillón's "MCS" Haar nose cascade (Castrillón et al., 2007) is not reliable, possibly because of the decision to use 18x15 pixel samples - we believe that this is too small. Its unequivocal success rate is below 50% for the reference dataset described above, as even when it finds exactly one "nose", it might be an eye, a forehead or a cheek rather than a nose.

By adding common-sense pruning rules (the nose is the one below the eyes and above the mouth) it is possible to improve the success rate.

Table 1 shows the number of regions found by the MCS nose cascade both without and with pruning rules. It should be remembered that the number of nose-like regions found is an upper bound on the number of successes, and the true number of successes is lower, as we shall see in Section 4.

Table 1: Results (MCS cascade).

Regions	MCS	MCS & pruning
0	545	545
1	2361	2720
2	343	15
3	29	-
4	2	-

When successful, the MCS nose cascade typically returns a rectangle which is 30% of the width and 25% of the height of the face. The mid-point is typically 60% down from the top of the face. Resolving any remaining ambiguity by choosing the one nearest this ideal position is usually correct.

The images in Figure 2 were the nose regions returned by applying the MCS nose cascade to Figure 1 (blurred to remove speckling). As the red lines superimposed on these images show, for frontal noses, the nose tip is close to the centre of the nose region, but for profile noses, it is not; this is typical. Statistically, the rule that the nose tip can be found at the centre of the nose region is reasonably reliable, but the cases where it fails are those where it is needed most.

In assessing the reliability of nose tip predictions, we compare the prediction with our known nose labellings. Errors of ± 1 pixel in any direction are to be expected and count as success. Errors of up to ± 4 pixels are regarded as "near misses" - the method has found the correct area but has not located it accurately. Errors greater than ± 4 pixels suggest that the method has not found the correct area and are regarded as failure. Of our labelled images, the centres of the nose-like regions found by the MCS nose cascade, pruned as described earlier, are: 146 (29%) successful, 277 (55%) near misses, and 79 (16%) failures.

If Haar cascades are to be used for finding nose tips, it seems necessary to treat frontal and profile noses separately, but this is not always straightforward. Sometimes, the distinction between frontal and profile noses is clear. Figure 1a is clearly frontal. Figure 1b is clearly profile. But what of Figure 1c? We classify this as a profile nose, as part of the nose feature is self-occluded, but in terms of its general appearance, it looks more like a frontal nose.

3.2 Random Ferns

A *Fern* (Ozuysal et al., 2010) is a hint as to the likely location of a feature. Individual ferns need not be reliable - as long as there are many of them and they are mutually independent, the consensus is reliable (Cao et al., 2012). Cao recommends Ferns chosen at random, with the area from which they are chosen shrinking gradually as the estimate of the position of the feature improves.

The conceptual similarities between Haar Features and Ferns are clear: both are weighted sums of pixel intensity difference operations (2 or 3 such operations for Haar Features, a configurable number, optimally 5, for Ferns).

The main differences between Haar Features and Ferns are:

- Haar Features are intended for use in sequences, to take advantage of adaptive boosting; Ferns are intended for use concurrently, using a voting method to choose between their various predictions
- Haar Features are created and analysed systematically; Ferns are drawn from an initial pool chosen randomly. (As a consequence, creation of Fern is much faster.)
- The chosen pixels in Ferns can be anywhere; the chosen pixel sums in Haar Features are always those of adjacent rectangles. (As a consequence, Ferns are more flexible.)
- The chosen pixels in Ferns can even be in other regions of the image; the chosen rectangles in Haar Features are always within the feature patch.
- Ferns are chosen according to their performance in positive samples; Haar Features are chosen according to their performance in both positive and negative samples.

We argue that, while both methods have advantages and disadvantages, it is clear which is which. If speed is crucial, the exhaustive analysis of Haar Features is a disadvantage, but the use of adaptive boosting is an advantage. The flexibility of Ferns is a clear advantage over the inflexibility of Haar Features, but Cao's choice of including pixels from other regions of the image in Ferns makes them vulnerable to changes of lighting conditions, so is a disadvantage. And the use of negative as well as positive samples when evaluating Haar Features is clearly beneficial.

Thus, while Haar Features have their deficiencies, abandoning them entirely in favour of Cao's approach is not the way to go.

We might also add a theoretical objection to Cao's idea. It is true that, as the initial pool of Ferns was created randomly, they are mutually independent. But the selection process is not random, it is based on image data, and this introduces mutual dependence within the final pool of selected Ferns, and we cannot guarantee that a consensus of mutually dependent recommendations is better than any individual recommendation. We shall return to this idea in the next section.

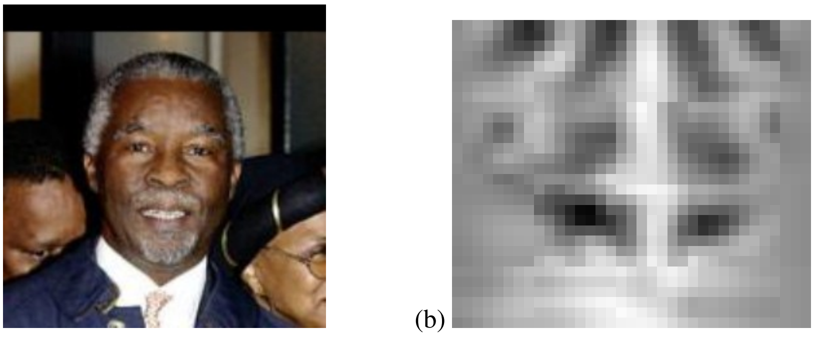

(a) (b)

Figure 3: A Symmetrical Nose (a) Original Image, (b) Self-Symmetry Output.

3.3 Hand-crafted Ferns

"Hand-crafted" ferns are the product of intelligent observation rather than random selection (and (Cao et al., 2012) deprecates their use for this reason). To some extent, they can be considered to be related techniques in the same general category as Haar Cascades and Random Ferns, inheriting the best aspects of both: as self-contained units, they can be used in sequence or in parallel; their creation and analysis can be as systematic as their designer chooses; and while rectangular groups of pixels are faster to process than random pixels, the rectangles need not be adjacent.

In this section, we discuss some ideas. Implementation recommendations and numerical results are to be found in Section 4.

One idea which could find the nose tip is simply to pick the brightest part of the nose region, on the reasoning that as the nose sticks out furthest from the face plane, it is most likely to catch the light, as can be seen in Figures 2b and 2c.

Working on the same lines, the brightness gradient down from the tip of the nose should be steepest, as the base of the nose is occluded and dark. This is still vulnerable to teeth and cheeks, and if the nose region is too large, it can even detect the white of the eye.

A related idea is to locate nostrils at the darkest two patches of the region and work from there. Preliminary results suggest that this is very sensitive to lighting conditions. One of the nostrils is usually the darkest patch in the region. For frontal noses, the second-darkest area could be anywhere - there is no consistency. For profile noses, the second-darkest region is so often the shadow of the wing of the darker side of the nose (as can be seen in Figure 2b) that this could be used as a reliable clue to the nose structure.

A combination of the previous two ideas, in which we compare the brightness of a single region with the darkness of two regions diagonally below it, has been found to be more successful than either.

For completeness, we also analysed a number of other options, the most successful of which was the inverse idea, comparing the brightness of a single region with the darkness of two regions diagonally above it. This too has merits - the depressions diagonally above the nose tip fail to catch the light.

The above ideas are clearly not mutually independent, as they all start by assuming a bright area (absolute or relative) around the nose tip. Ideally, we would wish to combine one or more of these with unrelated methods.

One independent idea would be to find the x-coordinate of the nose tip by finding a vertical plane of mirror symmetry through the nose region. Where the subject of the image has a particularly symmetrical nose (such as Figure 3a), self-symmetry of pixel intensities gives useful results (a clear, almost-vertical line can be seen in Figure 3b). However, this idea is particularly sensitive to lighting conditions and cannot be recommended.

We have also experimented with using self-symmetry of intensity gradients rather than self-symmetry of intensities. This was unsuccessful and has nothing to recommend it.

3.4 Other Methods

Artificial intelligence methods such as *Convolutional Neural Networks* could be used very effectively, as taking account of subtle cues elsewhere in an image is what they are good at, but using a CNN just to find a nose tip seems like overkill - finding the nose tip will be just one small component (albeit the most difficult to implement) of a much larger system.

Furthermore, the advantages of CNNs do not compensate for the practical disadvantage mentioned in Section 1. Retraining CNNs is slow and resource-intensive, often requires multiple-processor hardware, and can take hours or even days. For our purposes, a system which takes 30 minutes to retrain on a laptop computer and works adequately thereafter is better than a system which may work somewhat better

(a) (b) (c)

Figure 4: Problematic Face (a) Original Image, (b) Not a Nose (MCS), (c) Frontal Nose.

but could require 30 hours, or specialist hardware, or both.

4 INVESTIGATION

We have trained our own nose cascades using images taken from the LFW dataset and labelled by eye. We trained two cascades using positive samples with the nose tip at the centre, one for frontal noses and one for profile noses (using symmetrical cascades so as to allow for both left-facing and right-facing profile noses).

The frontal face cascade is sized at 25x17 pixels (see Section 4.1). It was created using 276 positive and 648 negative samples. It has 16 stages. It took 37 minutes to create on a home laptop. The profile face cascade is sized at 35x19 pixels - it is larger as it may have to contain the whole nose in little more than half of its region. It was created using 155 positive and 533 negative samples. It has 18 stages. It took 78 minutes to create on a home laptop.

When creating cascades, we used the entire primary dataset, plus additional images from the reference dataset as required to improve cascade performance. As labelling was by eye, nose tip position is often subjective and errors of ± 1 pixel are to be expected.

Builds are tested initially using the primary dataset, and successful builds are then tested more thoroughly using the reference dataset.

In addition, we have a “rogue’s gallery” of 10 faces (4 female, 6 male, including Figures 4a and 5a) which were particularly troublesome during development and which received special attention. These do not overlap with the primary dataset.

Numerical results for these cascades are to be found in Section 4.2. It is clear that, when both frontal and profile cascades find the same region, we need a better way of combining the two predictions, as either cascade alone is better at locating the nose tip than is combining the two.

While we were developing our cascades, it was the face shown in Figure 4a which gave the most false positives, both before and after pruning. MCS (Castrillón et al., 2007) finds just a single “nose” region for this face, the one shown in Figure 4b - unfortunately, however nose-like it may appear, this is his right cheek. The real nose, shown in Figure 4c, is one of several nose-like regions found by our cascades.

The face shown in Figure 5a is the one which currently gives the most false positives after pruning. MCS (Castrillón et al., 2007) finds two “nose” regions for this face, but the false one is pruned out, leaving the region shown in Figure 5b. Our cascades find more possibilities, including not only the one in Figure 5b but two in which one nostril and one fold of the cheek are interpreted as two nostrils, as shown in Figure 5c.

Even knowing that the nose is on the right-hand side of Figure 5c, it is hard not to interpret the feature on the left-hand side of the image as a second nose.

Pruning cheeks is not straightforward. Most of them lie within a bounding box formed from the outside edges of the eye regions and the edges of the mouth region, and many of them even lie within a bounding box formed from the centres of the eye regions and the edges of the mouth region. Shrinking the bounding box further could exclude many genuine noses.

Since our cascade combination finds the correct nose position (albeit alongside many false positives) and MCS does not, the result for Figure 4 must be counted as a modest success. But there is clearly much more work still to be done before we have a reliable nose-finder.

4.1 Cascade Region Size

In support of our belief that 18x15 pixels is too small, we offer the following analysis for frontal noses.

We created three frontal nose cascades, using the

Figure 5: Problematic Face (a) Original Image, (b) Nose Region (MCS), (c) Two Noses?

same 276 positive and 648 negative samples. The cascades were sized at 19x13, 25x17 and 31x21 pixels. The numbers of nose-like regions found by each of these cascades are shown in Table 2.

Table 2: Frontal Nose Cascades.

# Regions	19x13	25x19	31x21
0	1260	480	391
1	1275	985	452
2	562	879	569
3	157	551	568
4	22	241	468
5	4	106	359
6	-	29	211
7	-	9	138
8	-	-	66
9	-	-	30
10	-	-	17
11	-	-	9
12	-	-	2

Clearly, using larger patch sizes reduces the number of failures but increases the number of false positives. Our feeling is that 25x17 is optimal, and we hypothesise that this is because it is the typical size of noses in the LFW dataset - smaller sample sizes lose information, but larger sample sizes do not gain much information.

The effects on system performance will have to be tested during integration - perhaps, in our final system, we should have several cascades of different sample sizes prepared in advance, and choose between them according to the size of the face.

4.2 Combined Cascade Performance

Table 3 shows the numbers of nose-like regions found by (a) our profile nose cascade alone, (b) the combination of frontal and profile nose cascades without pruning, and (c) the combination with pruning. The key result is that the number of images with 0 nose-like regions is less than half of that using the MCS cascade.

Table 3: Profile and Combined Nose Cascades.

# Regions	Profile	Combined	+ Pruning
0	414	263	263
1	765	215	632
2	841	419	1832
3	642	552	443
4	363	512	87
5	178	453	22
6	49	324	1
7	23	242	-
8	4	140	-
9	1	88	-
10	-	47	-
11	-	13	-
12	-	7	-
13	-	3	-
14	-	1	-
15	-	0	-
16	-	1	-

4.3 Hand-crafted Ferns

We analysed the performance of a number of multiple-boxcar methods, all of which sum pixel intensities in square patches, and compared their performance with the simple ideas presented above. In order to ensure that they are independent of lighting conditions, we limited our investigations to pixel-intensity-difference operations (reducing dependence on lighting intensity) between boxcars which are (a) in horizontally-symmetrical patterns (reducing dependence on lighting direction) and (b) in which the brightest region spans the line of symmetry (regardless of lighting, the nose tip protrudes furthest from the face plane and will catch the light best). We present them in ascending order of complexity. Boxcar sizes are optimised for 250x250 images in which the face is about 110x110 pixels, and should be varied in proportion for larger or smaller faces. Results were obtained using combined frontal and profile nose cascades, with pruning, and 502 labelled noses.

Fern C is the idea already presented: the nose tip is at the centre of the region found by the Haar cascades. Of our 502 labelled noses, 153 (29%) were successful, 205 (39%) were near misses, and 144 (29%) were failures.

Fern B is a single boxcar: we find the brightest 9x9 square in the nose region. The nose tip is 7 pixels below the centre of the square. This Fern is based on the assumption that the nose tip will catch the light as it sticks out. Of our labelled noses, 67 (13%) were successful, 189 (38%) were near misses, and 246 (49%) were failures.

Fern D is a double-boxcar: we find the pair of 7x7 squares M and N where M is immediately above N which maximises $(\Sigma M - \Sigma N)$. The nose tip is 2 pixels below the centre of M. This Fern is based on the assumption that the bottom of the nose will usually be dark as lighting is usually from above. Of our labelled noses, 98 (20%) were successful, 147 (29%) were near-misses, and 257 (51%) were failures.

Fern V is a vertical triple-boxcar: we find the trio of 7x7 squares L, M and N where M is immediately below L and immediately above N which maximises $(2\Sigma M - \Sigma L - \Sigma N)$. The nose tip is 3 pixels below the centre of square M. The assumption behind this Fern is that even if the nose tip is not bright in absolute terms, it will nevertheless be brighter than its surroundings. Of our labelled noses, 87 (17%) were successful, 123 (25%) were near misses, and 292 (58%) were failures.

Fern H is a horizontal triple-boxcar: we find the trio of 9x9 squares L, M and N where L and N are immediately either side of M which maximises $(2\Sigma M - \Sigma L - \Sigma N)$. The nose tip is at the centre of M. The assumption behind this Fern is that even if the nose tip is not bright in absolute terms, it will be bright relative to its surroundings. Of our labelled noses, 57 (11%) were successful, 101 (20%) were near-misses, and 344 (69%) were failures.

Fern T is a triangular triple-boxcar: we find the trio of 7x7 squares L, M and N where the centres of L and N are 3 pixels below and 4 pixels either side of the centre of M which maximises $(2\Sigma M - \Sigma L - \Sigma N)$. The nose tip is at the centre of square M. This method is based on the assumption that nostrils are dark and are to be found either side of, and slightly below, the nose tip. Of our labelled noses, 185 (37%) were successful, 169 (34%) were near-misses, and 148 (29%) were failures. Fern T is by far the best of those based around a central bright square.

Fern U is an inverted triangular triple-boxcar: we find the trio of 11x11 squares L, M and N where the centres of L and N are 7 pixels above and 9 pixels either side of the centre of M which maximises $(2\Sigma M - \Sigma L - \Sigma N)$. The nose tip is 6 pixels below the centre of square M. This fern is based on the assumption that the depressions in the sides of the nose will be darker than their surroundings as they do not catch the light. Of our labelled noses, 61 (12%) were successful, 183 (36%) were near-misses, and 258 (52%) were failures.

Ferns are intended to be used together, and it is their team performance which is most important.

We combined the predictions of the two most successful ferns, C and T, using a weighted mean. We might expect both advantages and disadvantages: where one fern is right and the other is wrong, combining the two will be detrimental, but it can also happen that the two predictions are near-misses in opposite directions, and combining them results in an accurate prediction. In practice, the results are no better and no worse at accurate prediction than *Fern T* (although the binary prediction is slightly better at converting failures to near-misses): 185 (37%) are successful, 173 (34%) are near-misses, and 144 (29%) are failures.

What we want is a neutral arbiter to adjudicate those cases where the predictions of Ferns C and T are significantly different. Unfortunately, this is what we lack: all of our other Ferns are biased towards *Fern T*, as they all assume a bright square around the nose tip.

In terms of individual performance, the next-best Ferns are D and V, but these both include dark pixels below the nose which are also included in *Fern T*. They are not neutral arbiters. Thus the ternary combination we tested combined *Fern C* with Ferns T and U; these two may share the same bright region, but the dark regions do not overlap.

The three predictions were combined as follows: (a) weight all predictions according to how reliable the method is; (b) find the weighted mean of all predictions; (c) reweight the predictions according to how close they are to the mean; and (d) recalculate the weighted mean using the recalculated weights.

The results showed a slight decrease in accurate prediction, but an increase in near-misses: 180 (36%) were successful, 183 (36%) were near-misses, and 137 (27%) were failures. This can be explained as the third fern doing its job successfully when the two leading ferns make widely-different predictions, but contributing its own (worse) prediction when the two leading ferns are already close.

For the time being, we recommend using either *Fern T* alone (for speed), or combining this with *Fern C* (for somewhat better ability to avoid failures). If we are to make further progress, we need a new Fern which is independent of both.

5 CONCLUSION

This remains work in progress: it raises more questions than it answers. Haar classifiers followed by "hand-crafted ferns" can usually find the nose tip, but are there other, faster, more accurate or more reliable ways? Is the nose tip the best feature to detect, or would other parts of the nose (bridge or nostrils) be better? To what extent can the nose alone determine head pose? - occluded nostrils mean the user is looking down, and prominent nostrils mean the user is looking up, but can this variation be detected with sufficient accuracy to be useful?

To some extent, our boxcar method combines the advantages of Haar Features and Random Ferns, but as a first attempt, it is unlikely to be optimal. A deeper study would be welcome, but this would require a return to first principles and is work for the future.

The results in Section 4 demonstrate that (a) our combined cascade fails less often than MCS (Castrillón et al., 2007), and (b) it does not insist on a wrong interpretation of problematic faces such as Figure 4a. This is progress. Nevertheless, there is clearly much more work still to be done before we have a reliable nose-finder.

The target for on-the-spot retraining has not been met, particularly for profile noses. While we are waiting for faster portable computers to become widespread, we may have to accept that on-the-spot retraining is limited to frontal noses.

ACKNOWLEDGEMENTS

The authors wish to acknowledge the project: "Setting up of transdisciplinary research and knowledge exchange (TRAKE) complex at the University of Malta (ERDF.01.124)", which is co-financed by the European Union through the European Regional Development Fund 2014–2020.

REFERENCES

Cao, X., Wei, Y., Wen, F., and Sun, J. (2012). Face alignment by explicit shape regression. In *CVPR*, pages 2887–2894.

Castrillón, M., Déniz, O., Hernández, M., and Guerra, C. (2007). Encara2: Real-time detection of multiple faces at different resolutions in video streams. In *Journal of Visual Communication and Image Representation Vol 18 No 2*, pages 130–140.

Caunce, A., Cristinacce, D., Taylor, C., and Cootes, T. F. (2009). Locating facial features and pose estimation using a 3d shape model. In *ISVC09*.

Cristina, S. and Camilleri, K. P. (2018). Unobtrusive and pervasive video-based eye-gaze tracking. In *Image and Vision Computing 74*, pages 21–40.

Huang, G. B., Ramesh, M., Berg, T., and Learned-Miller, E. (2007). Labeled faces in the wild: A database for studying face recognition in unconstrained environments. Technical Report 07-49, University of Massachusetts, Amherst.

Ishikawa, T., Baker, S., Matthews, I., and Kanade, T. (2004). Passive driver gaze tracking with active appearance models. In *Proceedings of the 11th World Congress on Intelligent Transportation Systems*.

Lienhart, R. and Maydt, J. (2002). An extended set of haar-like features for rapid object detection. In *Proceedings. 2002 International Conference on Image Processing volume 1*, pages I–900. IEEE.

Lu, F. and Chen, Y. (2016). Person-independent eye gaze prediction from eye images using patch-based features. In *Neurocomputing (NC)*.

OpenCV (2015). *Open Source Computer Vision Library*.

Ozuysal, M., Calonder, M., Lepetit, V., and Fua, P. (2010). Fast key-point recognition using random ferns. In *IEEE Transactions on Pattern Analysis and Machine Intelligence,32(3)*, pages 448–461.

Rahmad, C., Andrie, R., Putra, D., Dharma, I., Darmono, H., and Muhiqqin, I. (2020). Comparison of viola-jones haar cascade classifier and histogram of oriented gradients (hog) for face detection. In *IOP Conference Series: Materials Science and Engineering. 732. 012038*.

Sapienza, M. and Camilleri, K. P. (2014). Fasthpe: A recipe for quick head pose estimation. Technical Report TR-SCE-2014-01, University of Malta.

Viola, P. and Jones, M. (2004). Robust real-time face detection. In *International Journal of Computer Vision, 57(2)*, pages 137–154.

Weidenbacher, U., Layher, G., Bayerl, P., and Neumann, H. (2006). Detection of head pose and gaze direction for human-computer interaction. In *Perception and Interactive Technologies. PIT*.

Zhang, Y. (2016). *Eye tracking and gaze interface design for pervasive displays*. PhD thesis, University of Lancaster.